

# We are IntechOpen, the world's leading publisher of Open Access books Built by scientists, for scientists

4,400

Open access books available

117,000

International authors and editors

130M

Downloads

Our authors are among the

154

Countries delivered to

TOP 1%

most cited scientists

12.2%

Contributors from top 500 universities



WEB OF SCIENCE™

Selection of our books indexed in the Book Citation Index  
in Web of Science™ Core Collection (BKCI)

Interested in publishing with us?  
Contact [book.department@intechopen.com](mailto:book.department@intechopen.com)

Numbers displayed above are based on latest data collected.  
For more information visit [www.intechopen.com](http://www.intechopen.com)



# Investigating the Structure-Related Properties of Cellulose-Based Superabsorbent Hydrogels

*Christian Demitri, Marta Madaghiele, Maria Grazia Raucci, Alessandro Sannino and Luigi Ambrosio*

## Abstract

Superabsorbent hydrogels are macromolecular networks able to absorb and retain large amounts of water solutions within their fine mesh-like structure. More importantly, they are capable of multiple swelling/shrinking transitions in response to specific environmental cues (*e.g.*, pH, ionic strength, temperature, presence of given electrolytes), thus exhibiting a stimuli-sensitive behavior, which makes them appealing for the design of smart devices in a number of technological fields. In particular, in the last two decades, cellulose-based superabsorbent hydrogels have proven to be an environmentally friendly and cost-effective alternative to acrylamide-based products. This chapter reviews the relationship between the molecular structure of cellulose-based hydrogels and their physicochemical properties. First, the network formation through the use of different cellulose derivatives and chemical or physical crosslinking agents is presented. Successively, the smart swelling capability of the hydrogels as a function of composition and structure is thoroughly discussed. Finally, several approaches to the hydrogel characterization are reviewed, with focus on the assessment of key mechanical, thermal and morphological properties.

**Keywords:** smart hydrogels, cellulose, characterization

## 1. Introduction

A superabsorbent hydrogel is defined as a three-dimensional (3D) matrix formed by hydrophilic polymers in linear or branched configuration and showing the ability to absorb large quantities of water or biological fluids (usually more than 100 grams of water per gram of dry polymer) [1].

The main property of superabsorbent hydrogels is the capability to preserve the stability of their network structure, even in the swollen state and in different media and environments. This feature is the result of the presence of crosslinking nodes [2], which can be induced through two main pathways, chemical and physical crosslinking. The former allows obtaining irreversible covalent bonds among the polymeric chains, *e.g.*, by radical polymerization, reaction of complementary groups, grafting reactions and enzymatic reactions [3]. The latter, instead, leads to the formation of reversible hydrogels, meaning that the matrix can be destroyed in specific environments, since the polymeric chains are held together only by physical

interactions, such as electrostatic attractions, entanglements, Van der Waals forces and hydrogen (H)-bonds [4].

The method adopted for crosslinking, either chemical or physical, also influences some key network properties (*i.e.*, water uptake capacity, swelling kinetics, mechanical and rheological properties, degradation rate, porosity, toxicity) and, consequently, the potential use of superabsorbent hydrogels in different fields [5]. Applicative sectors include, but are not limited to, agriculture, horticulture, hygienic products, wastewater treatment, water blocking tapes and tissue engineering [6, 7]. Therefore, depending on the intended use, the synthesis of hydrogels must be tailored to obtain materials that exhibit the desired responses, *e.g.*, fast swelling, degradability, porosity, *etc.*

Recently, particular focus has been placed on the production of novel superabsorbent hydrogels based on natural polysaccharides such as cellulose, starch and chitosan [8, 9], due to the low cost, biodegradability, availability and renewability of these raw materials. Compared to synthetic polymers (*e.g.*, polyacrylates), polysaccharides allow increasing the biocompatibility, biodegradability and water holding capacity of superabsorbent hydrogels, while decreasing their potential toxicity.

Being susceptible to degradation by microorganisms [10] and by chemical or physical stimuli [11], polysaccharide-based superabsorbent hydrogels are particularly suitable for use in soils as fully biodegradable systems for the controlled release of nutrients. However, although biodegradability permits to avoid the contamination of soils by chemicals, it may still represent a drawback in case of too early degradation, *i.e.*, when the nutrients inside the hydrogel matrix are not released as slowly as would be desired [12]. In fact, the total amount of nutrients should be released in a rate compatible with the plant necessity and occurring during the degradation time of the hydrogel matrix.

The most abundant polysaccharide in nature is cellulose, which has been the subject of academic and industrial studies for many years [13–15]. Although plant cellulose requires several purification steps to eliminate or reduce contaminants (*e.g.*, lignin and pectin), its large availability and low cost make it the preferred choice for the industrial-scale production of cellulose-based materials, including superabsorbent hydrogels. Conversely, the synthesis of cellulose by bacteria, such as *Acetobacter xylinum* and *Acanthamoeba castellanii*, yields a pure product but still on a laboratory scale, unsuitable for industrial uses. An additional source of cellulose may also be algae, *i.e.*, *Valonia ventricosa*, which provide highly crystalline material useful for studying polymorphs of the polymers [16].

In general, the strong hydrogen bonding (both intermolecular and intramolecular) among the hydroxyl groups along the cellulose backbone not only limits the water solubility, but also leads to the poor reactivity of cellulose. For this reason, great interest has been directed to the use of cellulose derivatives, also termed cellulose derivatives, such as ethyl cellulose, propyl cellulose and carboxymethylcellulose (CMC) [16]. In particular, sodium carboxymethylcellulose (CMCNa) is one of the most important water-soluble derivatives currently used, produced by chemical reaction between cellulose and monochloroacetic acid (MCA) in the presence of sodium hydroxide. CMC is widely applied as an additive in a variety of industrial sectors. Examples of products where CMC is used are detergents, oil drilling muds and wall paper glues, while high purity CMC grades are found in pharmaceuticals, tooth paste, cosmetics, food, *etc.*

With specific regard to agricultural applications and the need to control the hydrogel degradation in the soil, some studies reported the possibility to use binary systems based on two cellulose derivatives, *e.g.*, carboxymethyl and hydroxyethyl cellulose (CMCNa/HEC). Such binary systems have been shown to delay nitrogen release [17], improve soil moisture, reduce the use of water, and alleviate

environmental hazards caused by excessive fertilization. As an example, Sannino et al. have recently developed cellulose-based superabsorbent hydrogels [18] with sorption properties similar to those showed by conventional acrylate-based products, by crosslinking CMCNa and HEC in water solution with either divinylsulfone (DVS) or a water-soluble carbodiimide. Furthermore, the possibility to use a component of lemon juice, *i.e.*, citric acid (CA), as a natural cross-linker has been investigated [19]. In this case, the CA crosslinking of CMCNa and HEC, occurring at high temperature by means of an anhydride intermediate, allows to overcome the typical toxicity of chemical crosslinkers and to increase the hydrophilicity and roughness surface of the cellulose hydrogels, thus extending their potential to biomedical applications, including tissue engineering [20].

In this chapter, after a brief overview of the inherent features of cellulose and cellulose derivatives, the synthesis and characterization of cellulose-based hydrogels are discussed, with specific regard to CMCNa/HEC hydrogels, which represent a successful example of 'green' and biocompatible superabsorbents. The focus of the chapter is on the modulation of the physicochemical properties of the hydrogels in relation to their intended use, via changes to the molecular structure.

## 2. Cellulose backbone properties

The chemical and physical properties of cellulose and cellulose derivatives can be properly interpreted only after acquiring a deep knowledge of the cellulose molecule, in terms of chemical description, structure and morphology [21]. Generally, when approaching the study of macromolecules especially for the creation of crosslinked structures, three structural levels must be identified. The first one is the molecular level, which regards the single polymer chain and is characterized by the following structural parameters: chemical constitution, molecular mass and molecular mass distribution, reactive sites and intramolecular interactions. The second structural level to be identified is the supramolecular level, which accounts for the interactions (*i.e.*, packing, ordering) among macromolecules to form increasingly larger structures, such as elementary crystals, fibrils and fibers. Key structural parameters at the supramolecular level include the crystallinity degree, the degree of order within and around fibrils and the fibrillar orientation with respect to the fiber axis. Finally, the third level is the morphological one, dealing with complex structural entities formed by the macromolecules, *e.g.*, the distinct cell wall layers in native cellulose fibers and the presence of interfibrillar voids.

As highlighted in the following, the molecular and supramolecular levels are those of primary interest for the understanding of the structure-related properties of cellulose and its derivatives.

### 2.1 Molecular structure

Cellulose macromolecules are linear and rigid homopolymers consisting of D-anhydroglucopyranose units (AGU), linked together by  $\beta$ -(1  $\rightarrow$  4) glycosidic bonds formed between C-1 and C-4 positions of adjacent glucose moieties (**Figure 1**). The degree of polymerization (DP) of cellulose depends on both the cellulose source and the method of isolation/extraction. In general, plant cellulose in its native state has a DP higher than 10,000, which then drops down to 800–3000 following the extraction process [21].

The peculiarity of the glycosidic bond (**Figure 1**) is that the two AGU units joined together to form the repetitive unit of cellobiose are rotated by 180° with respect to each other [21]. The relative stiffness of the cellulose chain is partly

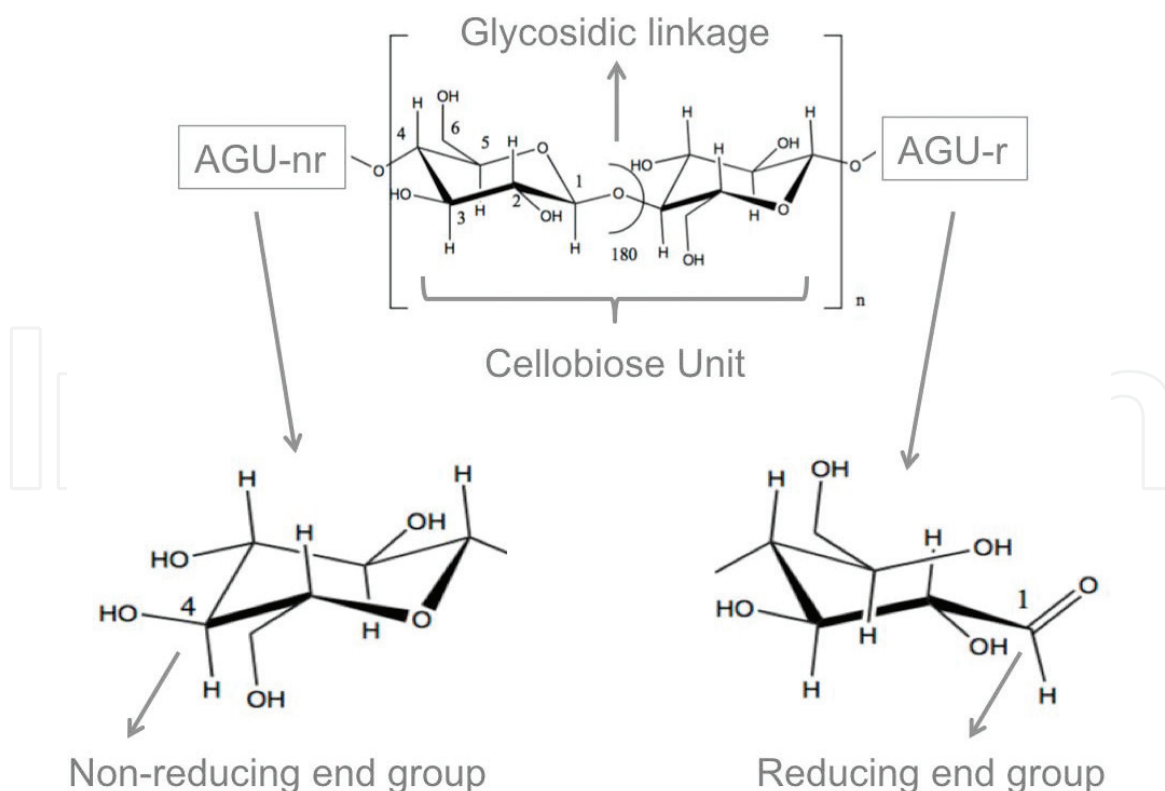


**Figure 1.**

*Molecular structure of cellulose representing the cellobiose unit with its reducing and non-reducing end groups.*

attributable to the steric constraints of the  $\beta$ -glycosidic linkage, as well as to the chair conformation of the pyranose ring. With focus on the terminal groups at either side of the cellobiose unit, an aldehyde hydroxyl (OH) group with reducing activity is found in C-1 position (**Figure 1**, right), whereas an alcohol-borne, non-reducing OH group is in C-4 position (**Figure 1**, left). Furthermore, both AGU units have three OH groups located at C-2, C-3 and C-6 positions (one primary and two secondary groups), which are mainly responsible for the poor reactivity and solubility of cellulose. Cellulose is indeed insoluble in water (although the  $\beta$ -glycosidic linkage is susceptible to hydrolytic attack), as well as in common organic solvents. This is due to the formation of an extensive intra- and inter-molecular hydrogen-bonding network among the abundant hydroxyl groups on the cellulose backbone. In particular, intramolecular bonding is ascribable to two different interactions, namely the one between the OH group at C-3 and the oxygen of the pyranose ring (first described in the 1960s by Marchessault and Liang), and the one between the C-6 and the C-2 OH groups of neighboring AGUs (reported by Blackwell et al. in 1977 [22, 23]). Intermolecular hydrogen bonding also takes place via the interaction between C-3 and C-6 groups of adjacent cellulose chains. Intramolecular bonds are those that mainly contribute to the stiffness of the cellulose molecule, which results in the high viscosity of cellulose solutions and the strong tendency of cellulose to crystallize and form fibrillar strands.

## 2.2 Functionalization

The hydroxyl groups located on the cellulose backbone (**Figure 1**) can be exploited for chemical modification to introduce various functionalities, with the aim of improving the solubility and the reactivity of cellulose. As aforementioned, a number of cellulose derivatives, which display a wide range of solubility in water and water solutions (in presence of alcohol or strong acids or bases), are commercially available in various industrial fields and used for a number of applications,

including coatings, laminations, optical films, absorbents, additives in building materials and also in pharmaceutical, food and cosmetic products [24–26]. Among these derivatives, the most important ones are esters and ethers (*e.g.*, cellulose acetate, methylcellulose, carboxymethyl cellulose and ethyl and hydroxyethyl cellulose), which are prepared on large-scale production by heterogeneous slurry reactions. These reactions most likely result in a random distribution of the substituents along the cellulose backbone. The degree of heterogeneity is determined by the deviations between experimentally measured substituent distributions in the monomers and ideal distributions, which are calculated under the assumption that the samples are prepared in ideal homogeneous reaction conditions [27].

With specific regard to carboxymethyl cellulose (CMC), which is widely used for the synthesis of superabsorbent hydrogels, the average degree of substitution (DS) and degree of polymerization (DP) of available CMC may vary considerably, although DS is generally between 0.5 and 1.5 [28]. In order to control the distribution of the functional groups in CMC, several synthetic pathways have been developed. In this regard, one pathway, developed by Fink et al. [29], includes stepwise etherification using aqueous NaOH solutions at low concentrations. Carboxymethylation is, thereby, primarily achieved in the non-crystalline regions of the cellulose structure [30].

In addition to esterification and etherification, periodate oxidation of the glycol group of glucopyranoside results in the formation of two aldehyde groups (dialdehyde cellulose) [31, 32], which are useful for introducing a variety of substituents such as carboxylic acid [33], hydroxyls [34], or imines [35, 36].

## 2.3 Degradation features

### 2.3.1 Effect of enzymes

It is well known that cellulose undergoes enzymatic degradation by specific enzymes, like cellulase and  $\beta$ -glucosidase. Direct physical contact between the enzyme and the surface of the cellulose molecules is a preliminary requirement to enzymatic hydrolysis [37–40]. Since cellulose is an insoluble and structurally complex substrate, this contact can be achieved only by diffusion of the enzymes into the cellulose structure [41]. Therefore, the ability of cellulolytic microorganisms (*Bacillus subtilis* and *Bacillus licheniformis* from bacteria, and *Pleurotus ostreatus*, *Pleurotus florida*, and *Trichoderma viride* from fungi) to degrade cellulose largely depends on the physicochemical characteristics of the specific substrate, which affect the diffusion process and, as a result, the degradation rate [42, 43]. The size and surface properties of the cellulose fibrils, as well as the space between microfibrils and cellulose molecules in the amorphous region, are fundamental factors affecting the permeability of the cellulolytic enzymes [44]. The degree of polymerization and the degree of crystallinity of the cellulose molecules are also important structural parameters that limit the rate of enzymatic degradation. The presence of cellulose contaminants (or components with which cellulose is associated) may also affect the degradability of the given substrate [44].

With focus on cellulosics, the nature, concentration and distribution of substituted groups clearly influence the process of enzymatic degradation, since the chemical substitution may impair the recognition of the substrate by the enzymes [42]. However, it is worth pointing out that the effect of chemical modification on enzymatic resistance is not simply proportional to the number of substituted units. Indeed, neighboring units can also be involved in the enzymatic attack. This is due to the fact that the recognition of polymeric substrates by an enzyme generally implicates the simultaneous involvement of multiple moieties in the polymer chain

[32, 45]. In an interesting study by Kim et al. [32], it has been shown that the chemical oxidation of cellulose not only makes the oxidized glucopyranosides enzyme-resistant (towards both cellulase and  $\beta$ -glucosidase), but also renders the adjacent unmodified glucopyranoside moieties inaccessible to the enzyme. Therefore, the enzyme-resistant portion of cellulose is much greater than the degree of oxidation when the latter is low, while becoming closer to the degree of oxidation when this is increased. The partial oxidation of cellulose can thus be a useful strategy for the design of cellulose-based materials, such as hydrogels, with predetermined degradation rates [32].

### 2.3.2 Effect of temperature

It is known that native cellulose exists as a mixture of two crystalline forms *Ia* and *Ib*, having triclinic and monoclinic unit cells, respectively [46, 47]. Cellulose *Ia* is thermodynamically less stable than *Ib*, as also demonstrated by its conversion at 260°C. In both crystalline forms, cellobiose is the repeating unit with a strong intra-chain H-bond, although the inter-chain H-bonding and packing of the crystal are different in the two forms [48].

Thermal degradation of cellulose is quite a complex phenomenon, involving several chemical reactions whose understanding still appears controversial [49]. At high temperatures (approximately above 250°C), thermal degradation occurs as a first-order reaction. Pyrolysis is thought to take place rapidly via transglycosylation reactions, which lead to the formation of anhydro-sugars or 'anhydrocellulose' [50].

Furthermore, while at high temperature the effect of oxygen on thermal degradation is practically negligible, at lower temperatures oxygen plays a predominant role, so that oxidative degradation in air proceeds faster than pyrolysis in nitrogen. The oxidative degradation process involves the production of free-radical initiators, which then interact with oxygen to lead to autocatalytic oxidative reactions, characteristic of the thermal oxidation of polymers [50].

Along with furanic compounds and gases (*e.g.*, carbon dioxide and carbon monoxide), water is a key product of the thermal degradation of cellulose. This is of great importance in cellulose degradation, as water can cause hydrolytic scission of the bonds between the glucosidic units, leading to diminished degree of polymerization and loss of physical properties [51]. While the physical elimination of water from cellulose occurs at low temperatures (approximately below 220°C), the chemical loss of water takes place in the range 220–550°C. Various chemical reactions have been proposed to explain the observed water loss in this temperature range. Water elimination from cellulose is primarily due to the formation of anhydrocellulose, as mentioned above, through both intra-ring and inter-ring dehydration mechanisms [51]. Intra-ring dehydration involves the intramolecular elimination of water from C-2 and C-3 OH groups, while inter-ring dehydration is due to OH groups from adjacent chains that form crosslinks perpendicular to the chain direction [52]. Another possible mechanism of intermolecular dehydration is a grafting reaction between the C-6 and C-4 OH groups of adjacent chains, leading to the formation of an ether bond [52]. High temperatures (>300°C) may induce further elimination of water from C-6, yielding a vinylene group. Secondary reactions such as ring rearrangement, following the initial elimination reaction, lead to further water loss and production of furanic species [51].

### 2.3.3 Effect of alkaline environment

Cellulose degradation strongly depends on the alkaline condition of environment. At temperatures <170°C the glycosidic linkages between the glucose units

are stable in alkaline conditions [53]. However, a dramatic decrease of molecular weight is observed when cellulose is boiled in presence of a diluted sodium hydroxide solution, even with the careful exclusion of oxygen.

The principal mechanisms of degradation in alkaline media have been described by several investigators [53, 54], and they include endwise degradation (or peeling) at temperatures  $<170^{\circ}\text{C}$  and alkaline hydrolysis of glycosidic bonds at higher temperatures. Endwise degradation is due to a number of isomerizations of the reducing end group of the cellulose molecule, which result in the migration of the carbonyl group along the carbon chain. The ketose or aldose end groups that are produced are then subjected to  $\beta$ -elimination [55]. If  $\beta$ -elimination occurs at the C-4 position, one monomer unit is released from the cellulose molecule, and the next glucose end group can take part in the reaction. In this way, the glucose units are gradually released from the macromolecule, resulting in a depolymerization process commonly known as *peeling-off reaction* or *unzipping reaction*. However, the  $\beta$ -elimination can also occur at positions other than C-4; in that case, the hexose unit remains attached to the cellulose molecule, which terminates the depolymerization. This is called the chemical *stopping reaction*. After either type of elimination reaction, a diketo intermediate is formed: this can undergo benzilic acid rearrangement, which generates the final degradation products. The two most common degradation products generated by peeling-off and chemical stopping reactions are epimers of 3-deoxy-2-C-(hydroxymethyl)-pentanoic acid (ISA) and 3-deoxy-hexanoic acid (metasaccharinic acid) [56].

When the temperature is  $>170^{\circ}\text{C}$ , random alkaline scission of glycosidic linkages occurs, resulting in considerable weight loss and marked decrease in degree of polymerization. It is reported that the reaction does not depend on the presence of molecular oxygen and is followed by peeling from any new reducing end group produced by the scission process, thereby resulting in much greater weight losses than alkaline degradation at lower temperatures [57]. Although alkaline scission is normally only associated with alkaline degradation at higher temperatures, it has been also observed in the alkaline degradation of amorphous hydrocellulose at temperatures  $<100^{\circ}\text{C}$ .

As mentioned for enzymatic degradation, the cellulose supramolecular structure plays a key role in the degradation process [58]. In general, a high supramolecular order of the polymer chains prevents or delays degradation [58, 59], with amorphous regions being much more sensitive to degradation than crystalline ones. It has been reported [53] that the rate-limiting step for slower chemical attack depends on the rate of mid-chain scission or the reaction of 'inaccessible' end groups. Peeling and chemical stopping are inhibited in fibrous hydrocellulose, which shows an ordered physical structure, and the majority of partially degraded molecules terminate with inaccessible reducing end groups, *i.e.*, by physical stopping. The relative rates of degradation (peeling) and stabilization (stopping) also depend on conditions such as the nature and concentration of the alkali and the temperature; stabilization is favored at high temperature and higher alkali concentrations [60].

### 3. Synthesis of cellulose-based hydrogels

Cellulosics are interesting precursors for the synthesis of superabsorbent hydrogels, due to the low cost, large availability, biocompatibility and biodegradability of cellulose, along with the responsiveness of some cellulosics (*e.g.*, CMCNa) to external stimuli.

In general, cellulose hydrogels can be stabilized via either physical (reversible) or chemical (irreversible) bonding of the cellulose chains, starting from dilute

aqueous solutions of single or composite cellulosic precursors [15]. Furthermore, natural and/or synthetic derived polymers might be combined with cellulose to obtain composite hydrogels with controlled properties [61, 62]. The number of crosslinking sites per unit volume of the network, called crosslinking degree, is a parameter that affects multiple properties of the hydrogel, including diffusive, mechanical and degradation properties. The control of the crosslinking degree, through adjustment of the synthesis protocol, thus represents a powerful tool to produce tunable hydrogels for the specific application at hand.

Commonly used physical hydrogels are those prepared from aqueous solutions of methylcellulose (MC) and/or hydroxypropyl methylcellulose (HPMC) [63]. The gelation process involves hydrophobic associations among the macromolecules via the methoxy group. While at low temperatures the polymer chains are well hydrated, at higher temperatures they start losing their bound water, so that polymer-polymer hydrophobic associations take place to form a 3D network. The sol-gel transition temperature clearly depends on the degree of substitution (DS) of the cellulose ethers and the presence of salts. A higher DS implies a more hydrophobic character of the cellulose chains, thus lowering the sol-gel transition temperature. Similarly, the addition of salts reduces the hydration level of the macromolecules. Both the DS and the salt concentration can be adjusted to obtain cellulose-based aqueous formulations able to gel at 37°C, for potential biomedical applications [64–66]. Several studies have addressed the use of low viscosity, injectable solutions, which may directly crosslink *in vivo* to deliver therapeutic molecules. However, the reversibility of physically crosslinked hydrogels, *i.e.*, their ability to flow or degrade under given circumstances (such as under mechanical loading) [67], still represents a significant limitation to their *in vivo* use. Conversely, *in vitro* applications of cellulose-based physical hydrogels appear much more attractive. In this context, MC hydrogels have been proposed as novel cell sheet harvest systems [66].

Unlike physical crosslinking, the formation of covalent bonding among the polymer chains creates a stable 3D network with given stiffness. Both physical treatments (*i.e.*, high-energy radiation) and chemical agents can be exploited to create irreversible cellulose-based networks. A number of chemical crosslinkers and catalysts are available to crosslink cellulose, including epichlorohydrin, aldehydes and aldehyde-based reagents, urea derivatives, carbodiimides and multifunctional carboxylic acids [15]. The crosslinking reactions may occur in water solution, organic solvents or in the solid state (*e.g.*, polycarboxylic acids can crosslink cellulose via condensation reactions occurring at high temperature) [19, 67–69]. It is important to emphasize that some crosslinking reagents, such as aldehydes, are highly toxic, thus impacting negatively on the biocompatibility and eco-sustainable character of cellulose-based hydrogels. Therefore, the use of non-toxic chemicals and/or physical processes is gaining increasing interest in the literature. In this regard, the recent crosslinking of CMCNa/HEC with citric acid has allowed the development of biocompatible, biodegradable and totally eco-friendly superabsorbent hydrogels [19].

Radiation crosslinking of cellulose, using electron beams or gamma radiation, appears also suitable for the production of biocompatible hydrogels, especially for biomedical applications. Although irradiation can lead to scission of the polymer backbone, as demonstrated also for cellulose [70], mild radiation conditions have been successfully adopted for the crosslinking and simultaneous sterilization of cellulose-based devices [71–73].

Finally, it is also important to highlight that cellulose backbone can be specifically functionalized before crosslinking, with the double aim of producing cellulose-based hydrogels free of potentially toxic contaminants as well as providing a higher

control of the crosslinking process. For instance, several cellulose derivatives have been added with acrylate moieties to enable the photo- or redox- crosslinking of aqueous solutions [74, 75]. Silylated HPMC, which crosslinks in solution by means of pH-driven condensation reactions, is another example of modified cellulose, proposed for the *in vivo* delivery of chondrocytes in tissue engineering applications [76, 77]. Tyramine-modified CMCNa has also been reported for the synthesis of enzymatically gellable formulations for cell delivery [78].

## 4. Smart swelling capability

### 4.1 Swelling ratio

The amount of water retained in the hydrogel network is a parameter of crucial importance, since it affects all the properties of the material that are relevant for the selected application (*e.g.*, stiffness, degradation, diffusion, biocompatibility, *etc.*). The hydrogel swelling is therefore the first property to be assessed; this is generally done by measuring the mass of solvent absorbed by the network:

$$Q_m = \frac{W_s - W_d}{W_d} = \frac{M_1}{M_2} \quad (1)$$

In Eq. (1),  $Q_m$  is the mass swelling ratio,  $W_s$  and  $W_d$  are the weights of the network in the swollen and dry state, respectively, while  $M_1$  and  $M_2$  indicate the masses of the solvent (*i.e.*, water) and the polymer, respectively.

The volume swelling ratio ( $Q$ ) can be calculated as follows:

$$Q = \frac{V_s}{V_d} = \frac{V_1 + V_2}{V_2} = 1 + Q_m \frac{\rho_2}{\rho_1} \quad (2)$$

where  $V_s$  and  $V_d$  are the volume of the swollen and dry state, respectively;  $V_1$  and  $V_2$  the volumes of water and polymer; and  $\rho_1$  and  $\rho_2$  their densities. The polymer volume fraction in the swollen state is given by:

$$V_{2,s} = \frac{1}{Q} \quad (3)$$

In general, the hydrogel absorption capacity depends on both internal parameters (related to the structure of the polymer network) and external parameters (related to the solution bathing the hydrogel). Superabsorbent hydrogels, in particular, are those that display intrinsic large sorption capabilities (with  $Q_m > 100$ ), together with a marked sensitivity to the external solution. This means that, by changing some environmental parameters (*e.g.*, pH, ionic strength), even slightly, superabsorbent hydrogels are able to undergo notable swelling/shrinking transitions [79].

### 4.2 Swelling mechanism

Superabsorbent hydrogels can be obtained by crosslinking hydrophilic polyelectrolyte species. Indeed, the presence of ions or fixed charges on the polymer network greatly improves its swelling behavior [80, 81].

Several factors governing the sorption mechanism can be identified. First of all, the polymer hydrophilicity promotes the polymer-solvent mixing, *i.e.*, the swelling,

when the material is placed in contact with water or water solutions. Secondly, there is the elastic retraction force due to the crosslinks, which opposes the swelling of the network. The entity of this elastic response clearly depends on the number of crosslinking nodes in the polymer network. In case of a perfect network with no dangling ends, loops, and entanglements, the number of elastically effective chain elements corresponds to the number of all chemically crosslinked polymer segments. The moles of polymer segments engaged by crosslinks and the moles of crosslinks per unit volume of the network are defined as the crosslink density and the degree of crosslinking, respectively. If  $\nu$  is the number of units engaged in crosslinks and  $V$  is the volume of the network, the crosslink density  $\rho_x$  is given by:

$$\rho_x = \frac{\nu}{V} = \frac{1}{\nu M_c} \quad (4)$$

where  $M_c$  is the number average molecular weight between two consecutive crosslinks and  $\nu$  is the specific volume of the polymer. Clearly, the higher  $M_c$ , the lower  $\rho_x$ ; consequently, a higher hydrogel swelling is expected at fixed environmental conditions.

In case of polyelectrolyte networks, two additional beneficial contributions to swelling occur: (a) an osmotic mechanism called ‘Donnan effect’, which is proportional to the number of ionic fixed charges on the hydrogel network and induces the penetration of water into the network to dilute its high charge concentration; and (b) the electrostatic repulsion between charges of the same sign on the polymer backbone, which tends to expand the network, thereby promoting the swelling.

The Donnan effect (also known as the Gibbs-Donnan effect) is related to the behavior of free charged particles in the presence of a semipermeable membrane separating two different solutions. Being the membrane semipermeable, only some charged species are able to pass through it in order to reach the equilibrium between the two solutions. A typical Donnan-type mechanism takes place when a 3D polyelectrolyte network is placed in contact with a water solution, since electrical charges are tethered on the polymer backbone, which thus acts as a semipermeable membrane. The equilibrium of the whole system (composed by the swelling solution and the polymer network itself) is attainable only if a passage of water is established, going from the external solution to the polymer network, thus diluting the concentration of the charges inside the network.

The polyelectrolyte nature of CMCNa explains why this cellulose derivative is widely used for the synthesis of superabsorbent cellulose-based hydrogels, especially in conjunction with HEC [13, 15, 18–20]. The simultaneous presence of HEC has been shown to be fundamental to achieve intermolecular (rather than intramolecular) crosslinking reactions, thus enabling the network stabilization [15]. The hydrogels crosslinked in presence of CMCNa clearly exhibit a much higher sorption capacity if compared with those crosslinked with HEC only, due to the Donnan-type swelling mechanism. The swelling capability of CMCNa/HEC hydrogels has been further increased by the use of difunctional molecules (*e.g.*, polyethylene glycol) as network spacers, able to increase the average distance between two crosslinking sites (*i.e.*,  $M_c$ ) [82].

#### 4.2.1 Effect of temperature

The hydrogel state can be considered as a peculiar solution composed of water and hydrophilic polymer chains. Because of the presence of crosslinks, which impede the polymer dissolution, the hydrogel solution is characterized by an elastic (rather than viscous) behavior [79].

The polymer-solvent interaction can be described by the thermodynamic theory of polymer solutions. In 1953, Flory [81] showed that the free energy change associated with the mixing process between the solvent and the polymer network can be calculated as follows:

$$\Delta G_{mix} = kT [n_1 \ln (1 - V_{2,s}) + \chi_{1,2} n_1 V_{2,s}] \quad (5)$$

where  $k$  is the Boltzmann constant,  $T$  the absolute temperature,  $n_1$  the number of solvent molecules, and  $\chi_{1,2}$  the Flory-Huggins polymer-solvent interaction parameter [81]. This last parameter takes on positive or negative values, for endothermic or exothermic mixing, respectively. In case of complete miscibility of the polymer in the solvent over the entire composition range,  $\chi_{1,2}$  is lower than 0.5. The exact value of this parameter can be calculated as follows:

$$\chi_{1,2} = \chi_a + \chi_b V_{2,s} + \chi_c V_{2,s}^2 + \dots \quad (6)$$

where  $\chi_a$ ,  $\chi_b$ , etc. are function of the temperature.

This means that the polymer-solvent interaction parameter, which in turn affects the polymer hydrophilicity and the hydrogel swelling, depends on temperature (and on polymer concentration). The effect of the temperature on  $\chi_{1,2}$  allows to design thermosensitive hydrogels. Most polymers increase their water solubility as the temperature increases (*i.e.*, the  $\chi_{1,2}$  parameter decreases), thus they are able to form positive temperature-sensitive hydrogels, which shrink upon cooling below their upper critical solution temperature (UCST). However, negative temperature-responsive hydrogels can be also obtained, which shrink when heated above their lower critical solution temperature (LCST), These include both physical systems, such as the MC and HPMC hydrogels discussed above [63–66], and chemical ones, for example obtained by copolymerizing cellulose derivatives with N-isopropylacrylamide [83].

#### 4.2.2 Effect of ionic strength (constant pH)

Polyelectrolyte networks (*e.g.*, CMCNa/HEC hydrogels) are able to significantly change their volume when changing the composition of the external solution. The fixed charges linked to the polymer backbone drive this peculiar response. In general, the equilibrium solution uptake always diminishes for higher values of the ionic strength. However, polyelectrolyte hydrogels display a marked sensitivity to ionic strength variations. This is due to the osmotic pressure related to the Donnan effect, which is proportional to the difference in concentration of charges between those contained in the gel and those in the external solution. Obviously, increasing the ionic strength of the external solution decreases the difference between the concentration of ion species in the gel and in the external solution and, as a result, the water uptake decreases. This behavior can be ascribed to the neutralization of the fixed charges linked to the polymer backbone by the “free” charges active in the external solution. This neutralization reduces the total active charge of the polymer network, thus reducing both the electrostatic repulsion of the polymer chains and the Donnan-type sorption mechanism. On the other hand, this effect can be explained as a reduction of the chemical potential of the water in the external solution, with a resulting reduction of its capability to penetrate the polymer network.

#### 4.2.3 Effect of pH (constant ionic strength)

In general, the degree of ionization  $i$  of polyelectrolyte chains depends on the dissociation constant of the ionizable network groups and the pH of the external

solution. In particular, anionic hydrogels (such as CMCNa/HEC ones) tend to deprotonate and swell when external pH is higher than  $pK_a$  of their ionizable groups, while cationic hydrogels protonate and swell when external pH is lower than  $pK_b$  of their ionizable groups.

The dissociation of the carboxylic groups fixed on the cellulose chains in CMCNa/HEC hydrogels is strongly affected by the pH of the external solution [18, 80]. A reduction in the number of dissociated carboxylic acid groups in the polymer network is evident at low pH. This mechanism reduces the swelling of the material, in accordance with the reduction of the polyelectrolyte property of the network. At very low pH values, the majority of the carboxylic acid groups are in a non-dissociated state, and the hydrogel seems to be composed of non-polyelectrolyte chains. On the other hand, when the pH of the swelling solution increases, there is a growth of the number of dissociated carboxylic group with a consequent increment in swelling.

## 5. Mechanical properties

The viscoelastic nature of polymers offers several analytical methods to investigate their mechanical behavior. In addition to 'traditional' mechanical tests (*e.g.*, tensile, compressive, flexural), dynamic mechanical analysis (DMA) is the method of choice to quantify the elastic (*i.e.*, conservative) and viscous (*i.e.*, dissipative) moduli of polymers,  $G'$  and  $G''$  respectively, in both the liquid and solid states. Basically, the method consists in subjecting the sample to a sinusoidal deformation, of given amplitude and frequency, and recording the double material's response in-phase (elastic) and out-of-phase (viscous) with the mechanical solicitation. With regard to gels, DMA is widely used to investigate both the progression of the crosslinking reaction and the mechanical properties of the final gel.

In general, the gelation of polymer solutions can be investigated by rheological and dynamic mechanical analyses. As the crosslinking reaction takes place, the viscosity of the polymer solution starts to increase progressively, due to the increase of the average molecular weight, until the gel state, defined as the one where no flow occurs (*i.e.*, infinite viscosity), is reached. Alternatively, the  $G'$  and  $G''$  moduli can be monitored during crosslinking via DMA, as a function of frequency, time or temperature [84, 85]. The initial polymer solution, characterized by a modulus  $G''$  higher than  $G'$ , undergoes a rapid increase of  $G'$  (higher and faster than the one of  $G''$ ) as the crosslinking reaction proceeds, so that the final gel state shows a modulus  $G'$  higher than  $G''$  for several orders of magnitude. The so-called gel point is defined as the one where  $G'$  and  $G''$  curves cross each other and basically it determines the temperature or the time required to obtain a gel from given solutions. In the literature, several investigations are reported exploring the physical or chemical gelation of cellulose-based hydrogels via DMA and are here suggested for further reading [84, 85]. In the following, instead, the authors address the mechanical characterization of final hydrogels, with particular focus on the relationship between the crosslink density and the stiffness of the polymer network.

Since hydrogels show a rubber-like behavior, the theory on the entropic elasticity of rubbers, described by Flory [81], can be exploited to estimate the degree of crosslinking of a hydrogel by measuring its macroscopic mechanical properties. Assuming that the deformation of the polymer chains is affine and that the volume of the polymer network does not change upon uniaxial deformation, Flory derived the following relationship between the uniaxial stress and the uniaxial deformation:

$$\sigma = RT\rho_{xe} \left( \alpha - \frac{1}{\alpha^2} \right) = G \left( \alpha - \frac{1}{\alpha^2} \right) \quad (7)$$

where  $\sigma$  is the stress,  $R$  is the universal gas constant,  $T$  is the absolute temperature,  $\rho_{xe}$  is the elastically effective crosslink density (*i.e.*, the number of elastically effective crosslinks per unit volume, which is equal to  $\rho_x$  for perfect networks),  $\alpha = L/L_i$  is the deformation ratio, with  $L$  the actual thickness of the deformed sample and  $L_i$  the initial thickness of the sample ( $\alpha > 1$  for elongation and  $\alpha < 1$  for compression, respectively), and  $G$  is the shear modulus of the polymer network. In practice, Eq. (7) holds for small deformations ( $\alpha \approx 1$ ), in order to assume a constant volume of the network, and states that the plot of  $\sigma$  against  $(\alpha - 1/\alpha^2)$  is linear, with a slope that is equal to the modulus  $G$  and directly proportional to the crosslink density.

If the polymer network is swollen isotropically in a solvent [81], and the crosslinking reaction occurs in the presence of the solvent [86], as for most hydrogels, the modulus  $G$  in Eq. (7) can be expressed as follows:

$$G = RT\rho_{xe} V_{2,s}^{1/3} V_{2,r}^{-1/3} = RT \frac{V_e}{V_0} V_{2,s}^{1/3} V_{2,r}^{2/3} \quad (8)$$

where  $V_0$  is the dry network volume,  $V_{2,s}$  is the polymer volume fraction in the fully swollen state (Eq. (3)), and  $V_{2,r}$  is the polymer volume fraction soon after crosslinking and before swelling, *i.e.*, in the relaxed state.

Therefore, the mechanical characterization of hydrogels via uniaxial elongation or compression tests allows estimating not only the gel stiffness and strength, but also the corresponding elastically effective crosslink density. However, it is worth recalling that, due to viscoelasticity, which implies a time-dependent material's response, the rate of gel loading is particularly important in the determination of its mechanical properties. Commonly used strain rates for hydrogel testing are in the range 1–50  $\mu\text{m/s}$  [87–90].

Although derived for uniaxial deformation, Eq. (8) has a general validity. DMA, which directly measures the modulus  $G$  through its components  $G'$  and  $G''$ , might thus be used also to estimate  $\rho_{xe}$  [87, 91]. Interestingly, for superabsorbent cellulose-based hydrogels, it has been demonstrated that the calculation of  $\rho_{xe}$  from both compression and DMA data provides comparable values, thus suggesting the high potential of DMA as a non-destructive method for the bulk mechanical characterization of hydrogels [87].

For selected types of hydrogels, especially those used in tissue engineering and cell culture applications, the determination of the local mechanical properties of the material, on the nano/submicron scale, is also of great interest for fully understanding the multiscale material behavior, as well as the cell response to the substrate stiffness or elasticity [90, 92]. Such local measurements can be performed via atomic force microscopy (AFM) and nanoindentation techniques [93]. Apart from its use for morphological surface analysis, in recent years AFM has emerged as a well-established method to map the nano-mechanical properties of elastic and viscoelastic materials [94], and to probe the elasticity of cells and biological tissues [92]. AFM can also be adapted to perform nanoindentation tests [94]. Several soft hydrated materials, such as hydrogels, have been characterized via AFM and/or nanoindentation and their local elasticity has been correlated to the bulk one [90, 92, 93]. Notably, the stiffness of single cellulose nanofibres in bacterial cellulose hydrogels has been very recently determined via AFM [95].

As a final consideration on the evaluation of mechanical properties, it is worth noting that Eqs. (7) and (8) are referred to the analysis of non-macroporous

hydrogels. The mechanical behavior of porous gels, which are briefly dealt with in a later section, is clearly affected not only by the precursor polymer(s) and the crosslink density, but also by porosity itself. The determination of the crosslink density of porous hydrogels from mechanical data should thus take into proper account the role of porosity. As for the assessment of the local mechanical properties, so far, AFM has been mostly used for probing of non-macroporous hydrogels, being the analysis of porous substrates particularly challenging. However, the mechanical characterization of porous hydroxypropyl cellulose methacrylate (HPC-MA) hydrogels by means of AFM has been successfully reported in recent literature [96]. The obtained elastic modulus, together with data from microstructural analysis, has also allowed the mechanical modeling of individual pores and the bulk scaffold [96]. These findings pave the way to a more extensive use of the AFM technique in the near future for the mechanical analysis of porous hydrogels.

## 6. Thermal stability

Thermal stability of hydrogels is commonly investigated by means of thermogravimetric analysis (TGA), a technique that allows identifying the temperatures at which sample weight losses occur, due to heating-induced transitions, such as evaporation of volatile substances (*e.g.*, moisture) and thermal decomposition. In particular, the first derivative of the TGA signal (DTG) is usually calculated to highlight the temperatures of maximum degradation. When comparing the TGA/DTG curve of given hydrogels with those of the respective precursors, very useful information can be obtained related to the quality and efficacy of the crosslinking reaction, as well as the overall stability of the synthesized polymer networks. With regard to cellulose-based hydrogels, the high number of cellulose derivatives and crosslinking protocols currently available for their synthesis (as discussed in the first part of this chapter) make it difficult to draw general or conclusive remarks on their thermal behavior. Therefore, in the following the thermal stability of cellulose-based hydrogels is briefly discussed with reference to specific examples reported in the literature [97, 98], where blends of CMCNa and HEC, used as hydrogel precursors, have been shown to exhibit higher or lower thermal stability in the crosslinked state compared to the native one, depending on the crosslinking protocol used.

### 6.1 TGA analysis of hydrogel precursors: CMCNa and HEC

As discussed in the previous sections, CMCNa and HEC are widely employed for the synthesis of superabsorbent hydrogels [87, 97–100]. In particular, CMCNa is the polyelectrolyte species that provides the hydrogels with enhanced swelling capability and sensitivity to environmental stimuli (*i.e.*, ionic strength and pH), thanks to the Donnan effect. HEC is adopted to promote the formation of intermolecular rather than intramolecular crosslinks, thus allowing the macromolecules to stabilize into a three-dimensional polymer network [87]. The synthesis of superabsorbent hydrogels, with sorption capabilities up to 500 times the dry weight, is commonly reported for CMCNa/HEC weight ratios of 2/1 and 3/1 (*i.e.*, when an excess of polyelectrolyte CMCNa is used) [87, 97].

When analyzing the thermal behavior of cellulose derivatives, it is worth recalling that, due to the major role of oxygen in cellulose degradation, especially at low temperatures (as discussed previously), the choice between air or nitrogen flow as an atmosphere in which performing the TGA analysis is fundamental and should always be specified.

For analyses in nitrogen flow, typical TGA/DTG curves for CMCNa and HEC (commonly reported in the range 25–500°C) basically show a two-step weight loss, with removal of moisture (up to 10% weight) in the temperature range 40–100°C, and rapid thermal degradation, mostly due to decarboxylation [101], in the range 230–300°C (about 40–50% weight) (**Figure 2**). Weight loss then slowly proceeds at higher temperatures due to further degradation mechanisms, such as those described in Section 2 (*e.g.*, water removal, cleavage of the glycosidic linkage, formation of furanic compounds). Maximum degradation temperatures for CMCNa and HEC have been reported to be 284 and 280°C, respectively [98].

## 6.2 TGA analysis of CMCNa/HEC hydrogels

As reported in the literature, CMCNa/HEC hydrogels may display two or more steps of thermal degradation, depending on the crosslinking agent(s) used [97, 98]. Additional steps of weight loss in the TGA curve, compared to the curves of cellulose precursors, may be indeed due to the degradation of the crosslinker molecules incorporated in the gel network. As an example, CMCNa/HEC (3/1) hydrogels, crosslinked by either fumaric or malic acid [98], have been recently shown to display a three-step degradation process, including: a first stage, occurring at low temperatures (up to 100°C), due to water/moisture evaporation; a second stage, in the range 200–270°C, related to decomposition of the crosslinker; a final stage, between 270 and 400°C, where thermal decomposition of cellulose backbone occurs. It is worth noting that, in this study, the hydrogels were found to possess a higher thermal stability than the corresponding cellulose precursors. In particular, increased hydrogel degradation temperatures were detected up to 298 and 317°C, when using increasing concentrations of malic and fumaric acid, respectively. This suggested the formation of highly stable cellulose networks upon crosslinking.

Clearly, such a finding is strictly related to the given crosslinking agent/reaction being investigated. For instance, in an independent investigation CMCNa/HEC hydrogels crosslinked by divinylsulfone (DVS) have been shown to be less thermally stable than native polymers [97]. The maximum degradation temperature of cellulose was indeed shifted from about 285 to 276°C, upon DVS crosslinking of a 5/1 CMCNa/HEC mixture. However, in that study the effect of different crosslinker concentrations on the hydrogel stability was not taken into account.

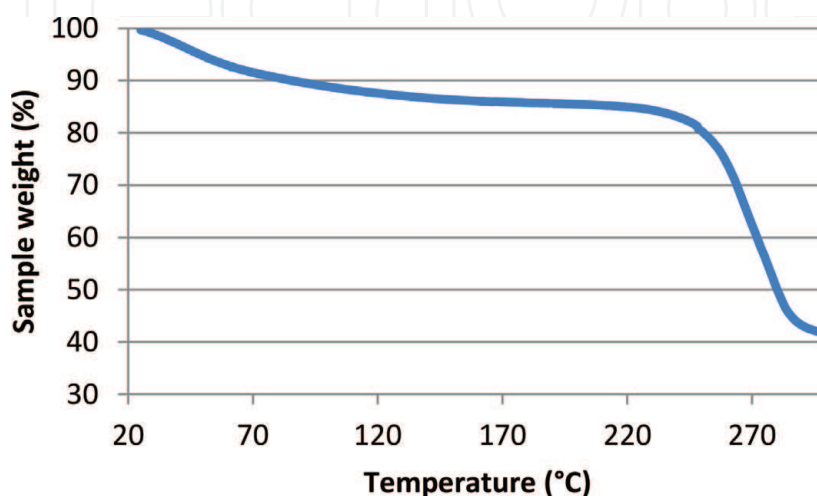


**Figure 2.**  
*Exemplificative TGA curve (25–300°C, nitrogen flow) obtained for a sample of HEC (unpublished data by the authors).*

## 7. Hydrogel morphology

In general, the analysis of hydrogel morphology (*i.e.*, porosity, at different length scales) is a fundamental characterization step for the full comprehension of most gel properties, including the thermodynamic and kinetic swelling behavior, the mechanical stiffness and strength and the diffusivity of molecules within the polymer network. However, such an investigation can be challenging, at least via standard experimental techniques (*e.g.*, microscopy), due to the inherent presence of water in the gel state.

In the following, the analysis of the gel structure is briefly discussed, with particular reference to the evaluation of pores at the nano-, micro- and macroscale. Where appropriate, specific examples related to the analysis of cellulose-based hydrogels are provided.

### 7.1 Nanoscale: hydrogel mesh size

Hydrogel networks show a fine mesh-like structure, where the free space among crosslinked chains can host the diffusion of water and other molecules of suitable size, smaller than or comparable to the mean hydrogel mesh size (**Figure 3**). According to the Canal-Peppas theory for isotropically swollen hydrogels [86], the average mesh size  $\xi$ , also referred to as correlation length, can be calculated from the following:

$$\xi = V_{2,s}^{-1/3} \left( \overline{r_0^2} \right)^{1/2} = V_{2,s}^{-1/3} l (C_n N)^{1/2} = V_{2,s}^{-1/3} l \left( C_n \frac{2M_c}{M_r} \right)^{1/2} \quad (9)$$

In Eq. (9),  $\left( \overline{r_0^2} \right)^{1/2}$  is the root-mean-squared end-to-end distance between adjacent crosslinks in the unperturbed state,  $V_{2,s}$  is the polymer volume fraction in the swollen state,  $l$  is the bond length along the polymer chain,  $C_n$  is the characteristic ratio of the polymer,  $N$  is the number of bonds per chain,  $M_c$  the molecular weight between crosslinks, and  $M_r$  the molecular weight of the polymer repeating unit. The higher the crosslink density (*i.e.*, the lower  $M_c$ ), the smaller the average mesh size. Typical  $\xi$  values for swollen hydrogels are reported in the range 5–100 nm [102, 103].

In spite of the fact that most real hydrogels show a broad range of mesh sizes, various studies show that the calculation of the average mesh size according to Eq. (9), starting from theoretical swelling or mechanical models for  $M_c$  determination, leads to a reliable and meaningful estimation of the hydrogel nanostructure [104, 105]. From an experimental point of view, the direct visualization or measurement of the hydrogel mesh size distribution is indeed hard to achieve. Standard microscopy techniques, including optical and electron microscopy, often require a too severe processing of the sample (*e.g.*, dehydration), which introduces numerous artifacts, thus deforming the structure of the gel with respect to its native state.

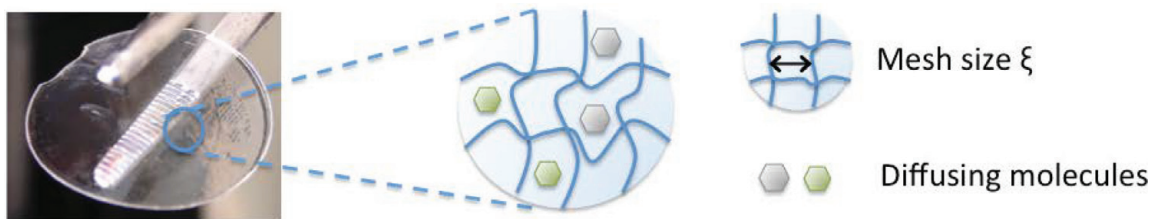


**Figure 3.** Schematic representation of a hydrogel network, with its average mesh size hosting multiple diffusing molecules.

Recently, some successful attempts have been made with cryo-transmission electron microscopy (cryo-TEM), for imaging various types of hydrogels (*e.g.*, methylcellulose hydrogels [106]) yet preserving their nanostructure [107, 108]. Cryo-TEM enables the high resolution imaging of the hydrogel under cryogenic conditions, showing the presence of vitrified water in a network of crosslinked polymeric chains. Nonetheless, it is obvious that the extreme care needed in sample preparation to avoid artifacts, still makes cryo-TEM poorly attractive for widespread use. Other methods to evaluate the hydrogel mesh size include confocal laser scanning microscopy (CLSM) [109], small-angle neutron scattering [106, 110, 111], small-angle X-ray scattering (SAXS) [104], pulsed field gradient [112] and low field nuclear magnetic resonance (NMR) spectroscopy [105]. Although accurate, these methods are based on expensive equipment and complex data analyses, which ultimately limit their application. Moreover, in many cases the estimated values of mesh size have been shown to be comparable with those calculated from theoretical models (Eq. (9)). This is why the indirect estimation of  $\xi$  via  $M_c$  determination (through swelling and/or mechanical tests) is by far the most widely employed method to study the hydrogel structure at the nanoscale. Further solute exclusion/diffusion experiments can be also performed to estimate the average mesh size from the diffusivity of molecules with given hydrodynamic radius [105, 113, 114], often confirming the average  $\xi$  values estimated theoretically.

With particular reference to cellulose-based hydrogels, it is worth mentioning thermoporosimetry as another interesting and powerful technique to measure the mesh size distribution, rather than the average mesh size, of polymer networks. The method, based on differential scanning calorimetry (DSC) and first described by Kunh et al. [115], relies on the application of the Gibbs-Thomson equation, which quantifies the freezing point depression of a liquid (*e.g.*, water), when confined in a porous medium, as inversely proportional to the pore size [116, 117]. Furthermore, the melting enthalpy is related to the pore volume, so that the entire mesh size distribution can be determined starting from the DSC curve [116, 117]. However, thermoporosimetry necessitates calibration against a known pore analysis method, proper adjustments of the DSC heating protocol for the given material being analyzed and signal deconvolution when the melting peaks of confined water and bulk water are overlapping [116]. For porous cellulosic materials, that show a low heat transfer and overlapping melting transitions, an isothermal step melting protocol has been recently proposed to estimate the pore size distribution through DSC analysis [116]. Moreover, since the DSC tracing of bound or confined water may be due to water-polymer interaction [118] rather than porosity confinement [119], preliminary experiments in various moisture environments have been suggested to verify whether porosity is the true factor governing the water melting behavior [120]. Several additional studies on the thermal behavior of water in cellulose-based materials are currently available in the literature and are here suggested for further reading [116, 118, 119], since they may provide useful information for the mesh size analysis of selected cellulose-based hydrogels via thermoporosimetry.

## 7.2 Micro- and macroscale: hydrogel porosity

For an environmentally sensitive hydrogel, the swelling rate, *i.e.*, the rate with which the hydrogel responds to external changes, is significantly affected by its bulk morphology. While reducing the size of the hydrogel in granular or powder form is a simple but rough method to accelerate its swelling kinetics, the creation of an interconnected network of micro- or macropores in the gel represents a sophisticated and accurate way to further control its bulk properties, including the swelling extent and kinetics. First of all, porous hydrogels can retain higher amounts of

water compared to non-porous ones, due to additional capillary retention [87, 99, 100]. Furthermore, they can rapidly swell or shrink in response to given stimuli, due to the convective water transport, taking place in the pore channels. Multiple synthesis methods have been proposed to produce porous hydrogels with given microstructure, which are generally based either on the use of a removable porogen/templating agent [121–123] or on the rapid expulsion of water by phase inversion in a non-solvent [87, 100]. Cryo-gelation, which consists of crosslinking a polymer solution at cryogenic temperatures, is a particular method where ice crystals are the interconnecting porogens, while the crosslinking reaction takes place in concentrated liquid microphases among them. Resulting cryogels exhibit a sponge-like form with remarkable properties compared to other types of porous, soft gels. Indeed, in addition to a very quick swelling/deswelling response, cryogels may also show high elasticity and shape memory, which can make them even injectable for specific biomedical applications [124, 125]. So far several cellulose-based porous hydrogels, including different types of cryogels, have been proposed in the literature as smart materials for a wide range of applications, *e.g.*, absorbents in the agriculture field [126], matrices for controlled drug release [127], stomach bulking agents [18] and scaffolds for tissue engineering [128].

The investigation of hydrogel porosity is primarily performed, with different levels of resolution, via optical methods, such as scanning electron microscopy (SEM) and CLSM, usually followed by software-based image analysis [122, 129]. As discussed above, particular caution is needed in sample preparation to avoid artifacts, especially in cases where preliminary sample dehydration is required (*e.g.*, in SEM). In this regard, cryo-SEM is particularly recommendable to visualize the structure of swollen hydrogels. Alternatively, freeze-drying may be exploited to preserve the gel structure as much as possible, before standard (*i.e.*, under high vacuum) SEM observation. Other methods to analyze the hydrogel porosity include mercury intrusion porosimetry [121] and X-ray computed microtomography ( $\mu$ CT) [123, 130, 131]. While the former still necessitates preliminary sample drying and may not be suitable for the analysis of very soft materials such as hydrogels,  $\mu$ CT represents a powerful and versatile technique for the quantitative analysis of hydrogel porosity. In general,  $\mu$ CT allows the non-destructive visualization and reconstruction of the entire 3D structure of a given material. Then, proper analysis of acquired images/sections provides significant morphological information such as the pore volume fraction and the pore size distribution [123, 130, 131]. Although  $\mu$ CT does not require particular care in sample preparation, in the case of porous hydrogels it is worth mentioning that long scanning times are often required to obtain good quality images, due to the typical low density of the materials. The presence of water in swollen hydrogels may further increase the scanning time, thus implying the simultaneous desiccation of the sample under the X-ray beam. The  $\mu$ CT analysis of freeze-dried hydrogels is thus recommended and is usually reported [130, 131]. Although the  $\mu$ CT quantification of porosity may be particularly challenging for some hydrogel-based materials, *e.g.*, cellulose-based ones, due to their very low density, the successful  $\mu$ CT characterization of various hydrogel types has been recently reported [123], thus suggesting the potential of the technique to be further refined for the analysis of a larger number of hydrogels.

## 8. Conclusions

Cellulose-based superabsorbent hydrogels are currently explored for a number of technological applications, which range from the traditional use of hydrogels as water absorbents in different contexts (*e.g.*, personal care products, agriculture) to

their latest use in both pharmaceutical and biomedical fields (e.g., controlled drug delivery, tissue engineering). The design of novel hydrogels requires a deep knowledge of the existing correlation between structure and properties of cellulose networks. Multiple cellulose derivatives can be synthesized and crosslinked, via different strategies, for the development of hydrogels with well-defined features, including the swelling capability and sensitivity to external stimuli, the degradation rate resulting from various environmental factors, the mechanical stiffness and strength, the mesh size and the diffusion of molecules within the hydrogel network, and the micro- and macroporosity. Depending on the intended application(s), various experimental tests, such as those briefly reviewed in this chapter, can be performed to highlight the properties of interest. Due to the large availability of cellulose, its environmentally friendly nature and its biocompatibility, it is reasonable to assume that cellulose and its derivatives will drive the evolution of smart hydrogels in different technological fields.

### Author details

Christian Demitri<sup>1\*</sup>, Marta Madaghiele<sup>1</sup>, Maria Grazia Raucci<sup>2</sup>, Alessandro Sannino<sup>1</sup> and Luigi Ambrosio<sup>2</sup>

<sup>1</sup> Department of Engineering for Innovation, University of Salento, Lecce, Italy

<sup>2</sup> Institute of Polymers, Composites and Biomaterials (IPCB), National Research Council of Italy, Naples, Italy

\*Address all correspondence to: [christian.demitri@unisalento.it](mailto:christian.demitri@unisalento.it)

### IntechOpen

© 2018 The Author(s). Licensee IntechOpen. This chapter is distributed under the terms of the Creative Commons Attribution License (<http://creativecommons.org/licenses/by/3.0/>), which permits unrestricted use, distribution, and reproduction in any medium, provided the original work is properly cited. 

## References

- [1] Chang C, Duan B, Cai J, Zhang L. Superabsorbent hydrogels based on cellulose for smart swelling and controllable delivery. *European Polymer Journal*. 2010;**46**:92-100
- [2] Pourjavadi A, Harzandi AM, Hosseinzadeh H. Modified carrageenan 3. Synthesis of a novel polysaccharide-based superabsorbent hydrogel via graft copolymerization of acrylic acid onto kappa-carrageenan in air. *European Polymer Journal*. 2004;**40**: 1363-1370
- [3] Hennink WE, van Nostrum CF. Novel crosslinking methods to design hydrogels. *Advanced Drug Delivery Reviews*. 2012;**64**:223-236
- [4] Ahmed EM. Hydrogel: Preparation, characterization, and applications: A review. *Journal of Advanced Research*. 2015;**6**:105-121
- [5] Fajardo AR, Silva MB, Lopes LC, Piai JF, Rubira AF, Muniz EC. Hydrogel based on an alginate-Ca<sup>2+</sup>/chondroitin sulfate matrix as a potential colon specific drug delivery system. *RSC Advances*. 2012;**29**:11095-11103
- [6] Raucci MG, Alvarez-Perez MA, Demitri C, Sannino A, Ambrosio L. Proliferation and osteoblastic differentiation of hMSCs on cellulose-based hydrogels. *Journal of Applied Biomaterials and Fundamental Materials*. 2012;**10**:302-307
- [7] Mekonnen T, Mussone P, Khalil H, Bressler D. Progress in bio-based plastics and plasticizing modifications. *Journal of Materials Chemistry A*. 2013;**1**: 13379-13398
- [8] Spagnol C, Rodrigues FHA, Pereira AGB, Fajardo AR, Rubira AF, Muniz EC. Superabsorbent hydrogel composite made of cellulose nanofibrils and chitosan-graft-poly(acrylic acid). *Carbohydrate Polymers*. 2012;**87**: 2038-2045
- [9] Wang WB, Wang J, Kang YR, Wang AQ. Synthesis, swelling and responsive properties of a new composite hydrogel based on hydroxyethyl cellulose and medicinal stone. *Composites Part B: Engineering*. 2011;**42**:809-818
- [10] Baldrian P, Valaskova V. Degradation of cellulose by basidiomycetous fungi. *FEMS Microbiology Reviews*. 2008;**32**:501-521
- [11] Villay A, de Filippis FL, Picton L, Le Cerf D, Vial C, Michaud P. Comparison of polysaccharide degradations by dynamic high-pressure homogenization. *Food Hydrocolloids*. 2012;**27**:278-286
- [12] Omidian H, Rocca JG, Park K. Advances in super porous hydrogels. *Journal of Controlled Release*. 2005;**102**: 3-12
- [13] Marcì G, Mele G, Palmisano L, Pulito P, Sannino A. Environmentally sustainable production of cellulose-based superabsorbent hydrogels. *Green Chemistry*. 2006;**8**:439-444
- [14] Pan A, Ragauskas AJ. Preparation of superabsorbent cellulosic hydrogels. *Carbohydrate Polymers*. 2012;**87**: 1410-1418
- [15] Sannino A, Demitri C, Madaghiele M. Biodegradable cellulose-based hydrogels: Design and applications. *Materials*. 2009;**2**(2):353-373
- [16] Heinze T, Liebert T. Unconventional methods in cellulose functionalization. *Progress in Polymer Science*. 2001;**26**:1689-1762
- [17] Ni B, Liu M, Lu S, Xie L, Wang Y. Environmentally friendly slow-release nitrogen fertilizer. *Journal of*

Agricultural and Food Chemistry. 2011;  
59:10169-10175

[18] Sannino A, Madaghiele M, Lionetto MG, Schettino T, Maffezzoli A. A cellulose-based hydrogel as a potential bulking agent for hypocaloric diets: An in vitro biocompatibility study on rat intestine. *Journal of Applied Polymer Science*. 2006;**102**:1524

[19] Demitri C, Del Sole R, Scalera F, Sannino A, Vasapollo G, Maffezzoli A, et al. Novel superabsorbent cellulose-based hydrogels crosslinked with citric acid. *Journal of Applied Polymer Science*. 2008;**110**:2453-2460

[20] Raucci MG, Alvarez-Perez MA, Demitri C, Giugliano D, De Benedictis V, Sannino A, et al. Effect of citric acid crosslinking cellulose-based hydrogels on osteogenic differentiation. *Journal of Biomedical Materials Research Part A*. 2015;**103**:2045-2056

[21] Granström M. Cellulose derivatives: Synthesis, properties and applications [Academic dissertation]. Helsinki University; 2009

[22] Machessault RH, Liang CJ. Infrared spectra of crystalline polysaccharides. III. Mercerized cellulose. *Polymer science*. 1960;**43**:71-84

[23] Blackwell JH, Kolpak F, Gardner K. Cellulose chemistry and technology. In: Arthur J, editor. ACS-Symp. Series No. 48. Washington: American Chemical Society; 1977. p. 42

[24] Haworth WN. The structure of carbohydrates. *Helvetica Chimica Acta*. 1928;**11**:534-548

[25] Haworth WN. Die Konstitution einiger Kohlenhydrate. *Berichte der Deutschen Chemischen Gesellschaft (A)*. 1932;**65**:43

[26] Staudinger H. Die hochmolekularen organischen Verbindungen—Kautschuk

und Cellulose. 2nd ed. Berlin: Springer Verlag; 1960

[27] Arisz PW, Kauw HJJ, Boon JJ. Substituent distribution along the cellulose backbone in *O*-methylcelluloses using GC and FAB-MS for monomer and oligomer analysis. *Carbohydrate Research*. 1995;**271**:1-14

[28] Bledzki A, Gassan J. Composites reinforced with cellulose based fibres. *Progress in Polymer Science*. 1999;**24**: 221-274

[29] Fink H-P, Dautzenberg H, Kunze J, Philipp B. The composition of alkali cellulose: A new concept. *Polymer*. 1986;**27**:944-948

[30] Heinze T. Feature article: New ionic polymers by cellulose functionalization. *Macromolecular Chemistry and Physics*. 1998;**199**:2341-2364

[31] Maekawa E, Koshijima T. Properties of 2,3-dicarboxy cellulose combined with various metallic ions. *Journal of Applied Polymer Science*. 1984;**29**: 2289-2297

[32] Kim U-J, Isobe N, Kimura S, Kuga S, Wada M, Ko J-H, et al. Enzymatic degradation of oxidized cellulose hydrogels. *Polymer Degradation and Stability*. 2010;**95**:2277-2280

[33] Kim U-J, Kuga S. Ion-exchange chromatography by dicarboxyl cellulose gel. *Journal of Chromatography. A*. 2001;**919**:29-37

[34] Casu B, Naggi A, Torri G, Allegra G, Meille SV, Cosani A, et al. Stereoregular acyclic polyalcohols and polyacetates from cellulose and amylase. *Macromolecules*. 1985;**18**:2762-2767

[35] Kim U-J, Kuga S. Thermal decomposition of dialdehyde cellulose and its nitrogen-containing derivatives. *Thermochimica Acta*. 2001;**369**:79-85

- [36] Kim U-J, Kuga S. Ion-exchange separation of proteins by polyallylamine-grafted cellulose gel. *Journal of Chromatography. A.* 2002; **955**:191-196
- [37] Robson LM, Chambliss GH. Cellulases of bacterial origins. *Enzyme and Microbial Technology.* 1989; **11**: 626-645
- [38] Beguin P. Molecular biology of cellulose degradation. *Annual Review of Microbiology.* 1990; **44**:219-248
- [39] Armstrong DW, Martin SM. Bacterial fermentation of cellulose: Effect of physical and chemical parameters. *Biotechnology and Bioengineering.* 1983; **11**:2567-2577
- [40] Baker JO, Adney WS, Thomas SR, Nives RA. Synergism between purified bacterial and fungal cellulases. *ACS Symposium Series.* 1995; **618**:114-149
- [41] Beguin P, Millet J, Chavaux S, Navas J. Bacterial cellulases. *Biochemical Society Transactions.* 1992; **20**:42-46
- [42] Beltrame PL, Carnitti P, Focher B. Enzymatic hydrolysis of cellulosic materials: A kinetic study. *Biotechnology and Bioengineering.* 1984; **31**:160-167
- [43] Lee YH, Fan LT. Kinetic study of enzymatic hydrolysis of insoluble cellulose: Analysis of the initial rate. *Biotechnology and Bioengineering.* 1982; **24**:2382-2405
- [44] Petre M, Zarnea G, Adrian P, Gheorghiu E. Biodegradation and bioconversion of cellulose wastes using bacterial and fungal cells immobilized in radiopolymerized hydrogels. *Resources, Conservation and Recycling.* 1999; **27**: 309-332
- [45] Teeri TT, Koivula A, Linder M, Wohlfahrt G, Divne C, Jones TA. *Trichoderma reesei* cellobiohydrolases: Why so efficient on crystalline cellulose? *Biochemical Society Transactions.* 1998; **26**:173-178
- [46] Atalla RH, Vanderhart DL. Native cellulose: A composite of two distinct crystalline forms. *Science.* 1984; **223**: 283-285
- [47] Kumar S, Gupta R, Lee YY, Gupta Ram B. Cellulose pretreatment in subcritical water: Effect of temperature on molecular structure and enzymatic reactivity. *Bioresource Technology.* 2010; **101**:1337-1347
- [48] Sinnott ML. Primary structure and conformation of oligosaccharides and polysaccharides. In: *Carbohydrate Chemistry and Biochemistry: Structure and Mechanism.* Cambridge, UK: RSC Publishing; 2007. pp. 140-288
- [49] Shen D, Xiao R, Gu S, Zhang H. The overview of thermal decomposition of cellulose in lignocellulosic biomass. In: Kadla J, editor. *Cellulose.* London, UK: IntechOpen; 2013. DOI: 10.5772/51883
- [50] Shafizadeh F, Bradbury AGW. Thermal degradation of cellulose in air and nitrogen at low temperature. *Journal of Applied Polymer Science.* 1979; **23**:1431-1442
- [51] Scheirs J, Camino G, Tumiatti W. Overview of water evolution during the thermal degradation of cellulose. *European Polymer Journal.* 2001; **37**: 933-942
- [52] Pastorova I, Arisz PW, Boon JJ. Preservation of d-glucose-oligosaccharides in cellulose chars. *Carbohydrate Research.* 1993; **248**:151
- [53] Knill CJ, Kennedy JF. Degradation of cellulose under alkaline conditions. *Carbohydrate Polymers.* 2003; **51**: 281-300
- [54] Theander O. In: Tipson S, Horton D, editors. *Advances in Carbohydrate*

Chemistry and Biochemistry. Vol. 46.  
San Diego: R. Academic Press; 1988.  
p. 273

[55] Bastone S. Development of conservation methods for the restoration of paper materials [PhD thesis]. University of Palermo; 2017

[56] Pavasars I, Hagberg J, Borén H, Allard B. Alkaline degradation of cellulose: Mechanisms and kinetics. *Journal of Polymers and the Environment*. 2003;**11**:39-47

[57] Richards GN. Alkaline degradation. In: Bikales NM, Segal L, editors. *High Polymers, Cellulose and Cellulose Derivatives*. Vol. V. New York: Wiley; 1971. pp. 1007-1014

[58] Askarieh MM, Chambers AV, Daniel FBD, FitzGerald PL, Holtom GJ, Pilkington NJ, et al. The chemical and microbial degradation of cellulose in the near field of a repository for radioactive wastes. *Waste Management*. 2000;**20**: 93-106

[59] Klemm D, Philipp B, Heinze T, Heinze U, Wagenknecht W. Degradation of cellulose. In: *Comprehensive Cellulose Chemistry, Fundamentals and Analytical Methods*. Vol. 1. Weinheim: Wiley; 1998. pp. 83-129

[60] Lai Y-Z, Ontto DE. Effects of alkalinity on endwise depolymerization of hydrocellulose. *Journal of Applied Polymer Science*. 1979;**23**:3219-3225

[61] Chen H, Fan M. Novel thermally sensitive pH-dependent chitosan/ carboxymethyl cellulose hydrogels. *Journal of Bioactive and Compatible Polymers*. 2008;**23**:38-48

[62] Chang C, Lue A, Zhang L. Effects of crosslinking methods on structure and properties of cellulose/PVA hydrogels. *Macromolecular Chemistry and Physics*. 2008;**209**:1266-1273

[63] Sarkar N. Thermal gelation properties of methyl and hydroxypropyl methylcellulose. *Journal of Applied Polymer Science*. 1979;**24**:1073-1087

[64] Tate MC, Shear DA, Hoffman SW, Stein DG, LaPlaca MC. Biocompatibility of methylcellulose-based constructs designed for intracerebral gelation following experimental traumatic brain injury. *Biomaterials*. 2001;**22**:1113-1123

[65] Stabenfeldt SE, Garcia AJ, LaPlaca MC. Thermoreversible laminin-functionalized hydrogel for neural tissue engineering. *Journal of Biomedical Materials Research. Part A*. 2006;**77**: 718-725

[66] Chen C, Tsai C, Chen W, Mi F, Liang H, Chen S, et al. Novel living cell sheet harvest system composed of thermoreversible methylcellulose hydrogels. *Biomacromolecules*. 2006; **7**(3):736-743

[67] Te Nijenhuis K. On the nature of crosslinks in thermoreversible gels. *Polymer Bulletin*. 2007;**58**:27-42

[68] Wang C, Chen C. Physical properties of the crosslinked cellulose catalyzed with nanotitanium dioxide under UV irradiation and electronic field. *Applied Catalysis A: General*. 2005;**293**(2B):171-179

[69] Coma V, Sebti I, Pardon P, Pichavant FH, Deschamps A. Film properties from crosslinking of cellulosic derivatives with a polyfunctional carboxylic acid. *Carbohydrate Polymers*. 2003;**51**(3): 265-271

[70] Charlesby A. The degradation of cellulose by ionizing radiation. *Journal of Polymer Science*. 1955;**15**(79):263-270

[71] Wach RA, Mitomo H, Nagasawa N, Yoshii F. Radiation crosslinking of methylcellulose and hydroxyethylcellulose in concentrated aqueous solutions.

- Nuclear Instruments and Methods in Physics Research Section B. 2003;**211**(4): 533-544
- [72] Liu P, Peng J, Li J, Wu J. Radiation crosslinking of CMC-Na at low dose and its application as substitute for hydrogels. *Radiation Physics and Chemistry*. 2005;**72**(5):635-638
- [73] Pekel N, Yoshii F, Kume T, Guven O. Radiation crosslinking of biodegradable hydroxypropylmethylcellulose. *Carbohydrate Polymers*. 2004;**55**(2): 139-147
- [74] Lin M-S, Chen A-J. Preparation and characterization of water soluble and crosslinkable cellulose acrylate. *Polymer*. 1993;**34**:389-393
- [75] Pal K, Banthia AK, Majumdar DK. Development of carboxymethyl cellulose acrylate for various biomedical applications. *Biomedical Materials*. 2006;**1**:85-91
- [76] Vinatier C, Magne D, Weiss P, Trojani C, Rochet N, Carle GF, et al. Silanized hydroxypropyl methylcellulose hydrogel for the three-dimensional culture of chondrocytes. *Biomaterials*. 2005;**26**:6643-6651
- [77] Vinatier C, Magne D, Moreau A, Gauthier O, Malard O, Vignes-Colombeix C, et al. Engineering cartilage with human nasal chondrocytes and a silanized hydroxypropyl methylcellulose hydrogel. *Journal of Biomedical Materials Research. Part A*. 2007;**80**: 66-74
- [78] Ogushi Y, Sakai S, Kawakami K. Synthesis of enzymatically-gellable carboxymethylcellulose for biomedical applications. *Journal of Bioscience and Bioengineering*. 2007;**104**:30-33
- [79] Tanaka T. Gels. *Scientific American*. 1985;**244**:124-136
- [80] Sannino A, Esposito A, De Rosa A, Cozzolino A, Ambrosio L, Nicolais L. Biomedical application of a superabsorbent hydrogel for body water elimination in the treatment of edemas. *Journal of Biomedical Materials Research. Part A*. 2003;**67**(3):1016-1024
- [81] Flory PJ. *Principles of Polymer Chemistry*. New York, Ithaca: Cornell University Press; 1953
- [82] Sannino A, Maffezzoli A, Nicolais L. Introduction of molecular spacers between the crosslinks of a cellulose-based superabsorbent hydrogel: Effects on the equilibrium sorption properties. *Journal of Applied Polymer Science*. 2003;**90**:168-174
- [83] Peng Z, Chen F. Synthesis and properties of temperature-sensitive hydrogel based on hydroxyethyl cellulose. *International Journal of Polymeric Materials and Polymeric Biomaterials*. 2010;**59**:450-461
- [84] Fatimi A, Axelos MAV, Tassin JF, Weiss P. Rheological characterization of self-hardening hydrogel for tissue engineering applications: Gel point determination and viscoelastic properties. *Macromolecular Symposia*. 2008;**266**:12-16
- [85] Desbrières J, Hirrien M, SB R-M. Thermogelation of methylcellulose: Rheological considerations. *Polymer*. 2000;**41**:2451-2461
- [86] Peppas NA, Merrill EW. Crosslinked poly(vinyl alcohol) hydrogels as swollen elastic networks. *Journal of Applied Polymer Science*. 1977;**21**:1763-1770
- [87] Sannino A, Pappadà S, Madaghiele M, Maffezzoli A, Ambrosio L, Nicolais L. Crosslinking of cellulose derivatives and hyaluronic acid with water-soluble carbodiimide. *Polymer*. 2005;**46**(25): 11206-11212

- [88] Herrick WG, Nguyen TV, Sleiman M, McRae S, Emrick TS, Peyton SR. PEG-phosphorylcholine hydrogels as tunable and versatile platforms for mechanobiology. *Biomacromolecules*. 2013;**14**:2294-2304
- [89] Madaghiale M, Marotta F, Demitri C, Montagna F, Maffezzoli A, Sannino A. Development of semi- and grafted interpenetrating polymer networks based on poly(ethylene glycol) diacrylate and collagen. *Journal of Applied Biomaterials and Fundamental Materials*. 2014;**12**(3):183-192
- [90] Tronci G, Grant CA, Thomson NH, Russell SJ, Wood DJ. Multi-scale mechanical characterization of highly swollen photo-activated collagen hydrogels. *Journal of the Royal Society Interface*. 2015;**12**:20141079
- [91] Madaghiale M, Piccinno A, Saponaro M, Maffezzoli A, Sannino A. Collagen- and gelatine-based films sealing vascular prostheses: Evaluation of the degree of crosslinking for optimal blood impermeability. *Journal of Materials Science. Materials in Medicine*. 2009;**20**:1979-1989
- [92] Engler AJ, Richert L, Wong J, Picart C, Discher DE. Surface probe measurements of the elasticity of sectioned tissue, thin gels and polyelectrolyte multilayer films: Correlations between substrate stiffness and cell adhesion. *Surface Science*. 2004;**570**:142-154
- [93] Ebenstein DM, Pruitt LA. Nanoindentation of soft hydrated materials for application to vascular tissues. *Journal of Biomedical Materials Research. Part A*. 2004;**69**:222-232
- [94] Tranchida D, Kiflie Z, Acierno S, Piccarolo S. Nanoscale mechanical characterization of polymers by atomic force microscopy (AFM) nanoindentations: Viscoelastic characterization of a model material. *Measurement Science and Technology*. 2009;**20**:095702
- [95] Gao X, Sozumert E, Shi Z, Yang G, Silberschmidt VV. Assessing stiffness of nanofibres in bacterial cellulose hydrogels: Numerical-experimental framework. *Materials Science and Engineering: C*. 2017;**77**:9-18
- [96] Abuelfilat AY, Kim Y, Miller P, Hoo SP, Li J, Chan P, et al. Bridging structure and mechanics of three-dimensional porous hydrogel with X-ray ultramicroscopy and atomic force microscopy. *RSC Advances*. 2015;**5**: 63909-63916
- [97] Astrini N, Anah L, Haryono A. Crosslinking parameter on the preparation of cellulose based hydrogel with divinylsulfone. *Procedia Chemistry*. 2012;**4**:275-281
- [98] Seki Y, Altinisik A, Demircioglu B, Tetik C. Carboxymethylcellulose (CMC)-hydroxyethylcellulose (HEC) based hydrogels: Synthesis and characterization. *Cellulose*. 2014;**21**: 1689-1698
- [99] Esposito F, Del Nobile MA, Mensitieri M, Nicolais L. Water sorption in cellulose-based hydrogels. *Journal of Applied Polymer Science*. 1996;**60**(13): 2403-2407
- [100] Sannino A, Madaghiale M, Conversano F, Mele G, Maffezzoli A, Netti PA, et al. Cellulose derivative-hyaluronic acid-based microporous hydrogels cross-linked through divinyl sulfone (DVS) to modulate equilibrium sorption capacity and network stability. *Biomacromolecules*. 2004;**5**(1):92-96
- [101] Samaha SH, Essa DM, Osman EM, Ibrahim SF. Synthesis and characterization of hydroxyethyl cellulose grafted copolymers and its application for removal of nickel ions from aqueous solutions. *International*

Journal of Engineering Innovation & Research. 2015;4:645-653

[102] Cruise GM, Scharp DS, Hubbell JA. Characterization of permeability and network structure of interfacially photopolymerized poly(ethylene glycol) diacrylate hydrogels. *Biomaterials*. 1998; **19**(14):1287-1294

[103] Lin CC, Metters AT. Hydrogels in controlled release formulations: Network design and mathematical modeling. *Advanced Drug Delivery Reviews*. 2006; **58**(12-13):1379-1408

[104] Waters DJ, Engberg K, Parke-Houben R, Hartmann L, Ta CN, Toney MF, et al. Morphology of photopolymerized end-linked poly(ethylene glycol) hydrogels by small-angle X-ray scattering. *Macromolecules*. 2010; **43**:6861-6870

[105] Kirchhof S, Abrami M, Messmann V, Hammer N, Goepferich AM, Grassi M, et al. Diels-Alder hydrogels for controlled antibody release: Correlation between mesh size and release rate. *Molecular Pharmaceutics*. 2015; **12**: 3358-3368

[106] Lott JR, McAllister JW, Arvidson SA, Bates FS, Lodge TP. Fibrillar structure of methylcellulose hydrogels. *Biomacromolecules*. 2013; **14**(8): 2484-2488

[107] Estroff LA, Leiserowitz L, Addadi L, Weiner S, Hamilton AD. Characterization of an organic hydrogel: A cryo-transmission electron microscopy and X-ray diffraction study. *Advanced Materials*. 2003; **15**:38-42

[108] Hule RA, Nagarkar RP, Altunbas A, Ramay HR, Branco MC, Schneider JP, et al. Correlations between structure, material properties and bioproperties in self-assembled b-hairpin peptide hydrogels. *Faraday Discussions*. 2008; **139**:251-264

[109] Watkins AW, Anseth KS. Investigation of molecular transport and distributions in poly(ethylene glycol) hydrogels with confocal laser scanning microscopy. *Macromolecules*. 2005; **38**: 1326-1334

[110] Hammouda B, Ho D, Kline S. SANS from poly(ethylene oxide)/water systems. *Macromolecules*. 2002; **35**: 8578-8585

[111] Matsunaga T, Sakai T, Akagi Y, Chung U-I, Shibayama M. Structure characterization of tetra-PEG gel by small-angle neutron scattering. *Macromolecules*. 2009; **42**:1344-1351

[112] Wallace M, Adams DJ, Iggo JA. Analysis of the mesh size in a supramolecular hydrogel by PFG-NMR spectroscopy. *Soft Matter*. 2013; **9**:5483

[113] Liao H, Munoz-Pinto D, Qu X, Hou Y, Grunlan MA, Hahn MS. Influence of hydrogel mechanical properties and mesh size on vocal fold fibroblast extracellular matrix production and phenotype. *Acta Biomaterialia*. 2008; **4**: 1161-1171

[114] Cavallo A, Madaghiele M, Masullo U, Lionetto MG, Sannino A. Photocrosslinked poly(ethylene glycol) diacrylate (PEGDA) hydrogels from low molecular weight prepolymer: Swelling and permeation studies. *Journal of Applied Polymer Science*. 2017; **134**: 44380

[115] Kunh W, Peterli E, Majer H. Freezing point depression of gels produced by high polymer network. *Journal of Polymer Science*. 1955; **16**:539

[116] Maloney TC. Thermoporosimetry of hard (silica) and soft (cellulosic) materials by isothermal step melting. *Journal of Thermal Analysis and Calorimetry*. 2015; **121**:7-17

[117] Nedelec J-M, Grolier J-PE, Baba M. Thermoporosimetry: A powerful tool to

- study the cross-linking in gels networks. *Journal of Sol-Gel Science and Technology*. 2006;**40**:191-200
- [118] Faroongsarng D, Sukonrat P. Thermal behavior of water in the selected starch- and cellulose-based polymeric hydrogel. *International Journal of Pharmaceutics*. 2008;**352**: 152-158
- [119] Nagamura K, Hatakeyama T, Hatakeyama H. Studies on bound water of cellulose by differential scanning calorimetry. *Textile Research Journal*. 1981;**51**:607-613
- [120] Kaewnopparat S, Sansernluk K, Faroongsarng D. Behavior of freezable bound water in the bacterial cellulose produced by *Acetobacter xylinum*: An approach using thermoporosimetry. *AAPS PharmSciTech*. 2008;**9**(2): 701-707
- [121] Sannino A, Netti PA, Madaghiele M, Coccoli V, Luciani A, Maffezzoli A, et al. Synthesis and characterization of macroporous poly(ethylene glycol)-based hydrogels for tissue engineering application. *Journal of Biomedical Materials Research. Part A*. 2006;**79**: 229-236
- [122] Chiu Y-C, Kocagöz S, Larson JC, Brey EM. Evaluation of physical and mechanical properties of porous poly(ethylene glycol)-co-(L-lactic acid) hydrogels during degradation. *PLoS One*. 2013;**8**(4):e60728
- [123] Ghafar A, Parikka K, Haberthur D, Tenkanen M, Mikkonen KS, Suuronen J-P. Synchrotron microtomography reveals the fine three-dimensional porosity of composite polysaccharide aerogels. *Materials*. 2017;**10**:871
- [124] Bencherif SA, Sands RW, Bhatta D, Arany P, Verbeke CS, Edwards DA, et al. Injectable preformed scaffolds with shape-memory properties. *PNAS*. 2012;**109**:19590-19595
- [125] Henderson TMA, Ladewig K, Haylock DN, McLean KM, O'Connor AJ. Cryogels for biomedical applications. *Journal of Materials Chemistry B*. 2013; **1**:2682-2695
- [126] Demitri C, Scalera F, Madaghiele M, Sannino A, Maffezzoli A. Potential of cellulose-based superabsorbent hydrogels as water reservoir in agriculture. *International Journal of Polymer Science*. 2013;**2013**:435073
- [127] Ciolacu D, Rudaz C, Vasilescu M, Budtova T. Physically and chemically cross-linked cellulose cryogels: Structure, properties and application for controlled release. *Carbohydrate Polymers*. 2016;**151**:392-400
- [128] Demitri D, Raucci MG, Giuri A, De Benedictis VM, Giugliano D, Calcagnile P, et al. Cellulose-based porous scaffold for bone tissue engineering applications: Assessment of hMSC proliferation and differentiation. *Journal of Biomedical Materials Research. Part A*. 2016;**104**: 726-733
- [129] Oelschlaeger C, Bossler F, Willenbacher N. Synthesis, structural and micromechanical properties of 3D hyaluronic acid-based cryogel scaffolds. *Biomacromolecules*. 2016;**17**:580-589
- [130] Göppert B, Sollich T, Abaffy P, Cecilia A, Heckmann J, Neeb A, et al. Superporous poly(ethylene glycol) diacrylate cryogel with a defined elastic modulus for prostate cancer cell research. *Small*. 2016;**12**(29):3985-3994
- [131] Cecilia A, Baecker A, Hamann E, Rack A, van de Kamp T, Gruhl FJ, et al. Optimizing structural and mechanical properties of cryogel scaffolds for use in prostate cancer cell culturing. *Materials Science and Engineering: C*. 2017;**71**: 465-472